Chimera state in delayed dynamics of a tunable semiconductor laser

Laurent Larger†, Bogdan Penkovsky†, Morgane Girardot-Poinsot† & Yuri Maistrenko‡

†FEMTO-ST / Optics department of Pierre-Michel Duffieux, UMR CNRS 6174, University of Franche-Comté
16 Route de Gray, 25030 Besançon Cedex, France
‡Institute of Mathematics and Center for Medical and Biotechnical Research, NAS of Ukraine
Tereschenkivska Str. 3, 01601 Kyiv, Ukraine
Email: llarger@univ-fcomte.fr, bpenkovs@univ-fcomte.fr, morgane.girardot-poinsot@edu.univ-fcomte.fr, y.maistrenko@biomed.kiev.ua

Abstract—Chimera states are exotic solutions arising in complex dynamics, typically in networks of coupled oscillators. They are characterized by a cluster arrangement within the network, each cluster being identified by a particular behavior of all of its individual oscillators. Chimeras appear thus as the occurrence of stable neighboring groups (the clusters) of oscillators, each oscillator motion being uniform within one cluster, but incongruent between clusters. We report the experimental, numerical, and theoretical observation of such virtual Chimera states in a particular class of complex dynamical system modeled by a nonlinear delay integro-differential equation. The corresponding experimental setup involves an optoelectronic delay oscillator in which the dynamical variable is the wavelength of a tunable laser diode.

1. Introduction

Chimera states in complex networks of coupled oscillators were first found numerically in 2002 [1], and then attracted great interest in the scientific community [2, 3]. Chimeras are typically observed in newtork of oscillators with so-called non-local coupling, meaning that not only nearest neighbors are interacting, but also more distant ones. Usually there are two bifurcation parameters used to detect the regions of Chimera existence in the network parameter space, the coupling strength and the coupling radius [3] (how far beyond the nearest neigbor should be the coupling distance between oscillators). The interest in this research area was again amplified in 2012 when the first experimental observations of Chimera states were succeeded in optics (transverse patterns in a light beam [4]), in chemistry (in a reactor with light catalysis [5]), and in mechanics (networks of metronomes distributed on mechanically coupled plateforms [6]). More recently the same phenomenon was identified for the first time in dynamics without spatial variable (thus calling them "virtual" Chimeras), i.e. in nonlinear delay dynamics [7], motivated by a space-time analogy for this delay dynamics proposed a long time ago [8].

In this latter context we were motivated to extend the electronic delay frequency modulation (FM) dynamics, to a conceptually similar photonic setup. We also provide here a discussion on the stability domain depending on time parameters of delay dynamics.

2. Experiment and modeling

Among the various fields in Physics and Biology involving dynamics modeled by differential equation with delay, Optics has proposed since the early 80s paradigmatic setups, among which the first experimental chaotic behavior have been found [10, 11]. Motivated by novel physical application concepts (optical chaos cryptography [12]), a specific optoelectronic nonlinear delayed oscillator has been proposed for the photonic generation of complex chaotic dynamics, which oscillator was involving laser wavelength fluctuations of a tunable semiconductor laser diode. Below in our experiment we will describe the concepts of this wavelength oscillator, adapting its properties to obtain the recently discovered "virtual" Chimeras as described in [7].

2.1. The nonlinear delayed in wavelength oscillator

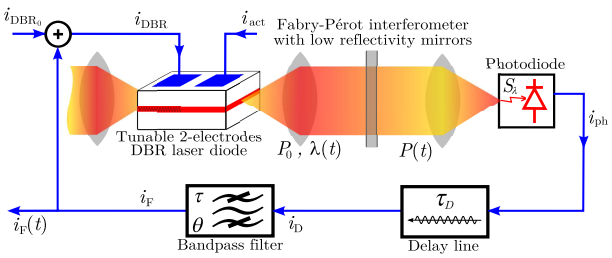

Figure 1: The nonlinear delay oscillator in laser wavelength

The block diagram of the experimental setup is represented in Fig. 1. It corresponds to an oscillator loop comprising of the following elements:

- A double-electrode laser diode with tunable wavelength, allowing to have a monochromatic light beam of power P_0, having the wavelength $\lambda = \lambda_0 + \delta\lambda$ proportional to the DBR section injection current i_{DBR}, continuously over a range $\Delta\lambda \simeq 1$ nm (with $\lambda_c \simeq 1550$ nm):

$$\lambda = \lambda_0 + \delta\lambda = \lambda_c + S_{\mathrm{DL}} \cdot i_{\mathrm{DBR}} \qquad (1)$$

- A Fabry-Pérot interferometer (FPI index $n = 1.5$, thickness $e = 5$ mm) of very moderate finesse (mirror with coefficient of reflection $R \simeq 50$ %), the role of which is to provide the nonlinearity through its transfer function between the output power $P(t)$ and the wavelength input $\lambda(t) = \lambda_c + \delta\lambda(t)$. The free spectral range (FSR= $c/(2n\,e)$) is selected to be smaller than the continuous tuning range of the laser (FSR $< \Delta\lambda$)

$$f_{NL}(x) = \frac{A}{1 + m \cdot \sin^2(x + \Phi_0)} = \frac{P}{P_0} \qquad (2)$$

$$\text{where } x = \frac{-2\pi ne}{\lambda_0^2}\,\delta\lambda \text{ and } \Phi_0 = \frac{2\pi ne}{\lambda_0}.$$

  In order to observe virtual Chimera, an essential feature of this nonlinear transformation consists in the asymmetry between the minima and maxima of the Airy function of the FPI. Indeed, with a transfer function derived from a 2-wave interferometer as in the original wavelength chaos photonic setup [12], the obtained $\sin^2$ – nonlinear function is perfectly symmetric, and does not allow to have "incongruent" clusters. It is also important to note that the parameter Φ_0 simply adjusted by a current offset i_{DBR_0} such as $\lambda_0 = \lambda_c + S_{DL} \cdot i_{DBR_0}$, allows to choose the operating point of the nonlinearity, around which the dynamics develops.
  The parameters A and m are conventionally defined for a Fabry-Pérot interferometer, $A = (1 - R)^{-1} \simeq 2$ and $m = 4R/(1 - R)^2 \simeq 8$ for $R \simeq 50$ %.

- A photodiode allows to convert, in a linear manner, the fluctuations of light intensity into the fluctuations of electric amplitude (i.e. a photo-current),

$$i_{ph} = S_\lambda \cdot P. \qquad (3)$$

- An electronic delay line, realized by FIFO memory (first in-first out, with a memory depth of N) is allowing to fine tune the value of the time delay via the clock frequency f_{CLK}, imposing the rythm at which the electronic signal is travelling through the memory:

$$i_D(t) = i_{ph}(t - \tau_D) \text{ where } \tau_D = N/f_{CLK}. \qquad (4)$$

- An electronic filter intended for the Fourier filtering performed by the electronic part of the oscillator. In the Fourier domain, this filter is described by a band-pass of filter with a gain H_0, a high cutoff frequency $f_h = (2\pi\tau)^{-1}$ and a low cutoff frequency $f_b = (2\pi\theta)^{-1}$:

$$H(\omega) = \frac{(i\omega\theta)\,H_0}{(1 + i\omega\theta)(1 + i\omega\tau)} = \frac{I_F(\omega)}{I_D(\omega)}. \qquad (5)$$

  The conversion rules between the Fourier and the time domains for this linear filter allow us to derive the following differential equation ruling the filter output $i_F(t)$ dynamics, given its input $i_D(t)$:

$$\frac{1}{\theta} \cdot \int_{t_0}^{t} i_F(\xi)\,d\xi + \left(1 + \frac{\tau}{\theta}\right) \cdot i_F(t) + \tau \cdot \frac{di_F}{dt}(t) = i_D(t) \qquad (6)$$

- Finally, an adder is used to define the average control current applied to the DBR electrode, which allows to determine the laser wavelength and thus the average operating point along the FPI modulation transfer function.

$$i_{DBR}(t) = i_{DBR_0} + i_F(t). \qquad (7)$$

2.2. Normalized dynamical model

The dynamics of the wavelength nonlinear delay oscillator can be now reduced from the description of each of the components of the oscillation loop by the physical equations (1-7). For the purposes of numerical simulation or analytical development, it is often appropriate to provide the evolution equation of our oscillator with normalized variables. Natural normalization of the dynamical variable is given by the dimensionless x argument involved in the Airy function (2). In terms of time, the delay is often considered as a time unit. This brings us to the following normalized model:

$$\delta \cdot \int_{s_0}^{s} x(\xi)\,d\xi + (1 + \varepsilon\,\delta) \cdot x(s) + \varepsilon \cdot \frac{dx}{ds}(s) = \frac{\beta}{1 + m \cdot \sin^2[x(s - 1) + \Phi_0]} \qquad (8)$$

where $s = t/\tau_D$ is the normalized time, $\delta = \tau_D/\theta = 2\pi f_b \tau_D$ and $\varepsilon = \tau/\tau_D = (2\pi f_h \tau_D)^{-1}$ are two (generally small) normalized parameters representing integral and differential weights in the dynamical process, $x = (-2\pi ne/\lambda_0^2) \cdot \delta\lambda = (-2\pi ne S_{DL}/\lambda_0^2) \cdot i_F$ is a normalized dynamical variable, actually proportional to the wavelength deviation, or also to the output signal of electronic filtering, $\beta = (-2\pi ne S_{DL} H_0 A S_\lambda/\lambda_0^2)$ is a normalized weight of the nonlinear delayed feedback, and finally $\Phi_0 = (2\pi ne/\lambda_c)(1 - S_{DL} \cdot i_{DBR_0}/\lambda_c)$ is a parameter allowing to choose, changing i_{DBR_0}, the operating point of the dynamics along the nonlinearity (according to (1) and (7) $\lambda_0 = \lambda_c + S_{DL} \cdot i_{DBR_0}$).
Unlike most delay equations (e.g. Ikeda or Mackey-Glass models), here we find an integral term early introduced in [13]. This term is a source of many unusual solutions in delay dynamics, such as *chaotic breathers* [14], harmonic solutions with high spectral purity [15], or stable square wave solutions with a single delay period [16]. A more conventional way to write the previous nonlinear integro-differential delay equation is to introduce an additional variable $y = \int x$. The following system of two first order

differential equations is obtained:

$$\varepsilon \frac{\mathrm{d}x}{\mathrm{d}s}(s) = -(1+\delta\varepsilon)\cdot x(s) - \delta \cdot y(s) + \frac{\beta}{1+m\,\sin^2[x(s-1)+\Phi_0]}, \quad (9)$$

$$\frac{\mathrm{d}y}{\mathrm{d}s}(s) = x(s).$$

δ and ε are generally small quantities under conditions corresponding to "large" delays, i.e. fast characteristic time τ is much smaller than the delay τ_D, and even longer integration time θ compared to the delay). This results in a product $\varepsilon\delta$ which is generally negligible (second order term) compared to 1, so that $(1+\varepsilon\delta)$ can be replaced by unity.

3. "Virtual" Chimeras

3.1. Spatio-temporal analogy

As already pointed out, the Chimera states are usually studied in networks of coupled oscillators. The delay dynamics, which we have just described, has *a priori* very different nature since it is a purely temporal system. Arecchi and coauthors [8] have however proposed first in 1992 a spatio-temporal analogy of delay dynamics which can help getting closer conceptually to the spatio-temporal dynamics of oscillator networks. The principle is to separate virtually the scales of multiple times actually involved in delay dynamics in order to assign the short time (of order τ, or ε) to a continuous "virtual space" variable σ, and also a long time (of order of delay τ_D, or a unit) to a discrete temporal variable n ($n \times \tau_D$ in physical units).

The trajectory of $x(s)$, solution of (9), can then be represented as a 2D graph $x(\sigma, n)$ where $\sigma \in [0, 1+\gamma]$ (with a small γ of order of ε) along horizontal dimension represents a virtual space variable describing changes in amplitude within a time interval corresponding to delay; The vertical axis of the 2D plot refers then to $n \in \mathbb{N}$ is a discrete time corresponding to an iteration of a time interval of (nearly, actually $(1+\gamma)\tau_D$) one delay interval to the next one. The normalized time s is thus decomposed according to these two spatial and temporal coordinates, $s = \sigma + n(1+\gamma)$.

Yet another way to describe our delay oscillator dynamics is via an integral formulation instead of differential one (8 or 9):

$$x(s) = \int_0^\infty h(\xi)\cdot f_{\mathrm{NL}}[x(s-1-\xi)]\,\mathrm{d}\xi, \quad (10)$$

where $h(s)$ is the impulse response of considered bandpass filter. With respect Chimeras in spatially extended dynamics of an oscillator network, a closer analogy can then be proposed compared: every "oscillator" of the network has an amplitude $x(s)$, which evolves dynamically in time corresponding to the discret time mapping of the intra-delay waveform, according to a nonlinear coupling through the function f_{NL} which is applied to the previous amplitude $x(s-1)$. However, from (10) it implies that this dynamics also depends on the amplitudes of neighbors on the distance of "ξ". According to this interpretation, $h(\xi)$ appears as a coupling coefficient of the "distance" function ξ to the considered oscillator. The non-local character of the coupling is revealed here as related to the spreading of the impulse response $h(s)$.

3.2. Results

The figure 2 illustrates the formation of Chimera state in a nonlinear delay dynamics both in experiment (figure 2(a)) and numerical simulation of the equation (9). Depending on parameters ε, δ, β as well as on initial conditions, one can obtain chimeras with one (top line) or multiple "heads" (bottom line, 2 heads). The time traces to the left of spatio-temporal representations (patterns in the (σ, n) plane) allow to assess the transitional phase of chimera state birth from initial conditions to the asymptotic chimeras states. In this latter case a virtual chimera has a head in the delay dynamics characterized by partitioning a time interval of a length very close to delay $(1+\gamma)$. There are two subintervals, one showing chaotic fluctuations (red and yellow colors) and other one stands for a plateau of constant amplitude (blue color). During the formation of two or more

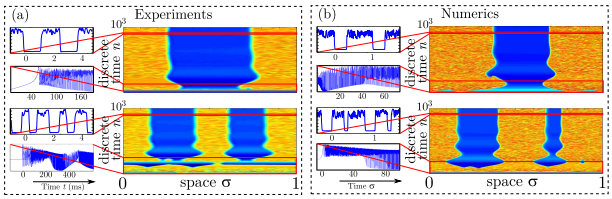

Figure 2: Appearance of Chimera in a delay dynamics with corresponding time traces and spatio-temporal representations. (a): Experiment, (b): Numerics. Amplitude values and gain parameters of the equation (9) are $\varepsilon = 5\text{x}10^{-3}$, $\delta = 8.4\text{x}10^{-3}$, $\beta = 1.0$, and $\Phi_0 = -0.35$.

chimeras heads, with the same parameter values for the dynamics, the "space" occupation ratio of chaotic amplitudes and the plateaus remains the same. Due to multistability of the system, initial conditions affect the number of "heads" observed.

Chimera formation occurs only within a specific area of the parameter space. When the gain β is insufficient, the dynamics reduces to a fixed point or a limit cycle of period 1 [16], or to slow motion periodic regimes dominated by the integral time scale (*chaotic breathers*). For higher gains a progressive transition to turbulence is observed, leading to fully developed chaotic regimes.

The temporal parameters δ and ε are equally important in the emergence of Chimera states. The standard scalar model of delay dynamics ($\delta = 0$) does not allow to observe

stable Chimeras [17]. The border of stable Chimera existence in the (ε, δ) plane is found to correpsond to the curve $\delta = \exp[(1 - \varepsilon^{-1})/2]$.

4. Conclusion

Delay dynamics is evolving in an infinite phase space and exhibits *a priori* a high potential for dynamic complexity, similar to spatio-temporal systems. From the experimental viewpoint the delay dynamics is much more simple to design and analyze through its purely temporal behavior. Basic signal processing techniques as well as flexible experiment tools in photonics offer high flexibility for the choice of various operating parameters and non-linear transformations. In this context we were able to demonstrate the existence of "Chimera" behavior in an optoelectronic oscillator with delayed feedback, which model is described by a nonlinear integro-differential delay equation.

This variety of behaviors confirms the well-known analogy to the networks of coupled oscillators in which "Chimera" states were initially identified.
It is interesting to mention that such an analogy was also exploited recently in an original application, a hardware implementation of a novel computational paradigm inspired by neural networks, which is a precisely a network of coupled oscillators [18, 19, 20].

References

[1] Y. Kuramoto and D. Battogtokh, Nonlinear phenomena in complex systems **5**, 380 (2002).

[2] D. M. Abrams and S. H. Strogatz, Phys. Rev. Lett. **93**, 174102 (2004).

[3] O.E. Omel'chenko, M. Wolfrum, and Y. Maistrenko, Phys. Rev. E **81**, 065201(R) (2010).

[4] A. M. Hagerstrom, T. E. Murphy, R. Roy, P. Hövel, I. Omelchenko and E. Schöll, Nature Physics (London) **8**, 658 (2012).

[5] M. Tinsley, S. Nkomo and K. Showalter, Nature Physics (London) **8**, 662 (2012).

[6] E.A. Martens, S Thutupalli, A. Fourrière, and O. Hallatschek, Proc. Nat. Acad. Sci., **110**, 26, 10563 (2013).

[7] L. Larger, B. Penkovskyi and Y. Maistrenko, Phys. Rev. Lett. **111**, 054103 (2013).

[8] F.T. Arecchi, G. Giacomelli, A. Lapucci and R. Meucci, Phys. Rev. A **45**, R4225 (1992).

[9] L. Larger, V.S. Udaltsov, and J.-P. Goedgebuer, Electron. Lett. **36** 199 (2000).

[10] K. Ikeda, Optics Commun. **30** 257 (1979).

[11] H.M. Gibbs, F.A. Hopf, D.L. Kaplan, R.L. Shoemaker, Phys. Rev. Lett. **46**, 474 (1981).

[12] J.-P. Goedgebuer, H. Porte and L. Larger, Phys. Rev. Lett. **80**, 2249 (1998).

[13] V.S. Udaltsov, L. Larger, J.-P. Goedgebuer, M.W. Lee, E. Genin, and W.T. Rhodes, IEEE Trans. Cir. Syst. I, **49** 1006 (2002).

[14] Y.C. Kouomou, P. Colet, L. Larger and N. Gastaud, Optics Letters, **32** 2571 (2007).

[15] Y.K. Chembo, L. Larger, H. Tavernier, R. Bendoula, E. Rubiola and P. Colet, Optics Letters, **32** 2571 (2007).

[16] L. Weicker, T. Erneux, O. D'Huys, J. Danckaert, M. Jacquot, Y. Chembo, L. Larger, Phys. Rev. E, **86** 055201(R) (2012).

[17] G. Giacomelli, F. Marino, M.A. Zaks and S. Yanchuk, Eur. Phys. Lett., **99** 58005 (2012).

[18] L. Appeltant, M.C. Soriano, G. Van der Sande, J. Danckaert, S. Massar, J. Dambre, B. Schrauwen, C.R. Mirasso and I. Fischer, Nature Commun., **2** 1 (2011).

[19] L. Larger, M.C. Soriano, D. Brunner, L. Appeltant, J.M. Gutierrez, L. Pesquera, C.R. Mirasso, I. Fischer, Optics Express, **20** 3241 (2012).

[20] Y. Paquot, F. Duport, A. Smerieri, J. Dambre, B. Schrauwen, M. Haelterman, and S. Massar, Scientific Reports, **2** 287 (2012).